Critical Interface: Poly-Silicon to Tunneling SiO_2 for Passivated Contact Performance

Preprint

William Nemeth,[1] Steve Harvey,[1] David Young,[1] Matthew Page,[1] Vincenzo LaSalvia,[1] Dawn Findley,[1] Abhijit Kale,[2] San Theingi,[1] and Pauls Stradins[1]

1 National Renewable Energy Laboratory
2 Colorado School of Mines

Presented at SiliconPV 2019
Leuven, Belgium
April 10–11, 2019

NREL is a national laboratory of the U.S. Department of Energy
Office of Energy Efficiency & Renewable Energy
Operated by the Alliance for Sustainable Energy, LLC

This report is available at no cost from the National Renewable Energy Laboratory (NREL) at www.nrel.gov/publications.

Contract No. DE-AC36-08GO28308

Conference Paper
NREL/CP-5900-73677
June 2019

Critical Interface: Poly-Silicon to Tunneling SiO_2 for Passivated Contact Performance

Preprint

William Nemeth,[1] Steve Harvey,[1] David Young,[1] Matthew Page,[1] Vincenzo LaSalvia,[1] Dawn Findley,[1] Abhijit Kale,[2] San Theingi,[1] and Pauls Stradins[1]

1 National Renewable Energy Laboratory
2 Colorado School of Mines

Suggested Citation
Nemeth, William, Steve Harvey, David Young, Matthew Page, Vincenzo LaSalvia, Dawn Findley, Abhijit Kale, San Theingi, and Pauls Stradins. 2019. *Critical Interface: Poly-Silicon to Tunneling SiO_2 for Passivated Contact Performance: Preprint*. Golden, CO: National Renewable Energy Laboratory. NREL/CP-5900-73677. https://www.nrel.gov/docs/fy19osti/73677.pdf.

NREL is a national laboratory of the U.S. Department of Energy
Office of Energy Efficiency & Renewable Energy
Operated by the Alliance for Sustainable Energy, LLC

This report is available at no cost from the National Renewable Energy Laboratory (NREL) at www.nrel.gov/publications.

Contract No. DE-AC36-08GO28308

Conference Paper
NREL/CP-5900-73677
June 2019

National Renewable Energy Laboratory
15013 Denver West Parkway
Golden, CO 80401
303-275-3000 • www.nrel.gov

NOTICE

This work was authored in part by the National Renewable Energy Laboratory, operated by Alliance for Sustainable Energy, LLC, for the U.S. Department of Energy (DOE) under Contract No. DE-AC36-08GO28308. Funding provided by U.S. Department of Energy Office of Energy Efficiency and Renewable Energy Solar Energy Technologies Office. The views expressed herein do not necessarily represent the views of the DOE or the U.S. Government. The U.S. Government retains and the publisher, by accepting the article for publication, acknowledges that the U.S. Government retains a nonexclusive, paid-up, irrevocable, worldwide license to publish or reproduce the published form of this work, or allow others to do so, for U.S. Government purposes.

Cover Photos by Dennis Schroeder: (clockwise, left to right) NREL 51934, NREL 45897, NREL 42160, NREL 45891, NREL 48097, NREL 46526.

Critical Interface: Poly-Silicon to Tunneling SiO_2 for Passivated Contact Performance

B. Nemeth[1, a)], S. P. Harvey[1], D.L. Young[1], M.R. Page[1], V. LaSalvia[1], D. Findley[1], A. Kale[2], S. Theingi[1], and P. Stradins[1]

[1.] *National Renewable Energy Laboratory, 15013 Denver West Parkway, Golden, CO USA, 80401*
[2.] *Colorado School of Mines, 1500 Illinois St, Golden, CO 80401*

[a)]Corresponding author: william.nemeth@nrel.gov

Abstract. Environmental exposure of our thin tunneling SiO_2 layer on nCz wafer samples prior to poly-Silicon (poly-Si) deposition critically impacts the resulting contact passivation. We present ToF-SIMS evidence of SiO_2 oxide storage-induced degradation, presumably by surface contaminants such as carbon, in symmetric and device poly-Si/SiO_2 lifetime samples as well as in finished cells. We also present methods to resurrect a contaminated SiO_2 layer, including UV-O_3 treatment prior to passivated contact formation to produce >21% TCO-free solar cells.

MOTIVATION AND BACKGROUND

Passivated contact-based silicon (Si) solar cells have shown the highest efficiency potential and are being intensively researched as the most likely next generation Si photovoltaic candidates beyond p-PERC. This approach is based on a thin passivating buffer layer between the silicon wafer and a carrier-selective conductive top layer. This thin insulator can either be amorphous silicon (a-Si:H[1]) or SiO_2[2], and it serves as a leaky dielectric layer that passivates dangling bonds on the wafer surface while still allowing carrier conduction.

The dielectric SiO_2 buffer layer is highly sensitive to post-formation processing leading to structural and compositional changes, while incorporation of impurities changes the nature of the interface. For example, carbon incorporated into SiO_2 may prevent blistering[3], the addition of nitrogen hinders B diffusion into SiO_2, while fluorine[4] promotes B diffusion into SiO_2 and helps to preserve passivation. Ozone applied to the SiO_2 layer can change its stoichiometry, reduces interface states[5], and removes impurities[6]. On the other hand, environmental contaminants attached to the SiO_2 surface might cause passivation loss. With a deeper understanding of the nature of surface contaminants, specific treatment regimens can be engineered to mitigate their negative effect. This would enable a wider processing window after SiO_2 formation prior to poly-Si deposition and result in: (1) more flexibility in environmental exposure, allowing collaborators to exchange samples with a methodology to maintain SiO_2 passivation and transport properties when incorporated into passivated contacts; and (2) manufacturers a way to mass-produce the SiO_2 based passivated contact cells with less stringent cleanliness or timing considerations.

EXPERIMENTAL PROCEDURE

A schematic of our all poly-Si passivated contact cell is shown in figure 1. The wafer is cleaned in SC-1 and SC-2 solutions, then subjected to a 700°C anneal in a tube furnace with a flowing N_2/O_2 mixture to grow the SiO_2 layer. Samples are then stored in polypropylene containers for one week in a mailing package in a car to simulate a transportation environment, while separate samples are stored in a N_2 box. This is followed by one of the following treatments: 1) SC-1 and SC-2 cleans without HF dips in an attempt to preserve SiO_2; (2) UV-O_3 exposure; (3) a deionized water rinse. Then, doped layers are deposited on the SiO_2 via 13.56 MHz RF plasma enhanced chemical vapor deposition as a-Si:H using SiH_4 and H_2 with PH_3 (for n-type) and B_2H_6 (for p-type) gases at 1 Torr. The resulting

device structures are then annealed in a tube furnace at 850°C to crystallize the a-Si:H into poly-Si. Next, atomic layer deposition (ALD) is used to deposit a sacrificial Al_2O_3 coating, which is annealed at 400°C to hydrogenate the structure. Al_2O_3 is then removed with dilute HF prior to evaporation of aluminum contacts and antireflective SiN_x deposition. The process sequence can be seen in figure 2 below. The minority carrier lifetimes are measured using a Sinton WCT-120 lifetime tester. Witness samples on polished wafers are characterized with nanometer resolved ToF-SIMS using 30 keV Bi primary and 1 keV Cs sputtering ions. J-V measurements are taken under 1-sun conditions on an inhouse tester using an official NREL Si reference cell for calibration on a temperature-controlled stage.

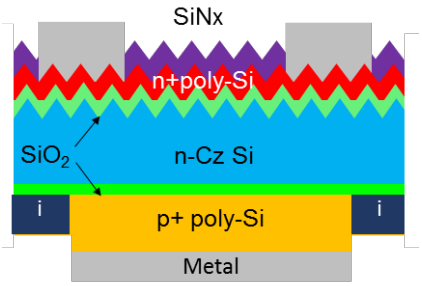

FIGURE 1. Schematic of rear emitter all poly-Si passivated contact cell.

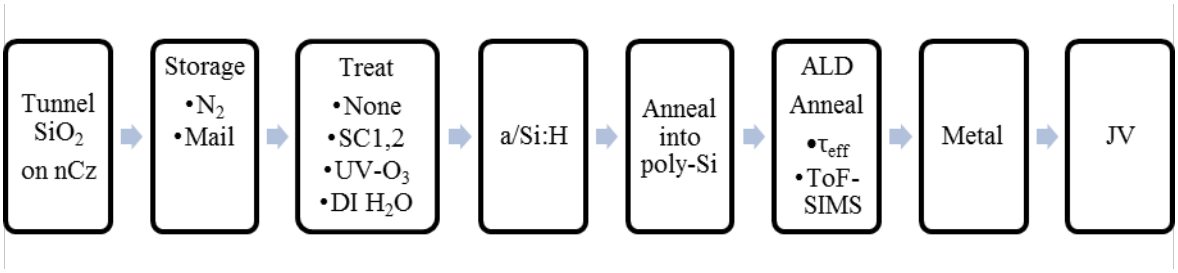

FIGURE 2. Process sequence for formation and treatment of passivated contact samples.

RESULTS AND DISCUSSION

As we developed our baseline poly-Si/SiO_2 cell process, we found substantial variations in lifetime and J-V characteristics, which were traced to the storage time between SiO_2 growth and subsequent a-Si:H deposition. This can be seen in figure 3 by the implied V_{oc} (iV_{oc}) extracted from lifetime measurements of several premetallized cells as a function of storage time in an N_2 environment. We find that the shorter duration of time to which the SiO_2 layer is exposed to a controlled N_2 environment prior to n/a-Si:H deposition results in better iV_{oc} values. Environmental contamination from metallic and/or organic sources as well as thickness changes to the SiO_2 layer may explain the differences. Likewise, symmetric p/poly-Si structures on planarized surfaces show similarly reduced lifetimes with longer exposure times for samples stored in an N_2 environment.

After cell metallization, the storage effect becomes even more pronounced (figure 4) as the V_{oc} drops to 450 mV (N_2 storage) and to 610 mV (mailing package storage). Post-storage treatment by SC-1 and SC-2 degrades performance by degrading the SiO_2 layer, but not as severely as the storage without any treatment. In contrast, a simple DI H_2O rinse as well as UV-O_3 exposure show a slight increase in iV_{oc} and a modest drop in V_{oc} coupled with an improvement in Fill Factor (FF). It is important to note that an increase in the thickness of the SiO_2 layer will decrease FF substantially due to decreased probability of tunneling, but we do not measure this and infer that the SiO_2 does not thicken. Using these treatments we were able to obtain TCO-free front/back poly-Si passivated contact cells of >20% (DI H2O) and >21% (UV-O_3) efficiencies. Notably, cells that received no post-storage treatment degraded significantly after metallization (figure 4 labelled N_2 storage and mail storage), while the treated cells did not show such a behavior. It should be noted that since the premetallized iV_{oc} was measured with an intact Al_2O_3 passivation layer, it is likely that this layer masks latent surface recombination centers such as pinholes or blisters in the poly-Si. Once the Al_2O_3 is removed and the structure is metallized, recombination active metal induced gap states are introduced.

We form our p/poly-Si passivated contact by first depositing a blanket i-layer, then a masked p-layer in a rear emitter configuration. Interestingly, the PL image (figure 5b) shows degradation only under the metallized p/poly-Si layer, while the perimeter i-layer retains passivation after removing the Al_2O_3 layer. Optical microscopic investigation reveals that 30 - 50 µm blisters (figure 5c) do exist in only the p/poly-Si regions, but not in i/ or n/poly-Si areas. This suggests that the boron diffusion may catalyze the aging-related degradation.

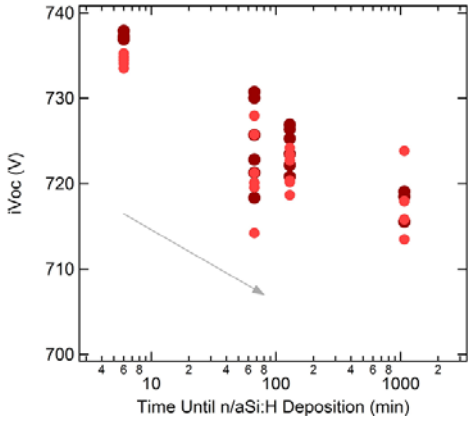

FIGURE 3. Pre-metallized cell iV_{oc} decrease with increasing storage time of SiO_2 in an N2 environment prior to n/a-Si:H.

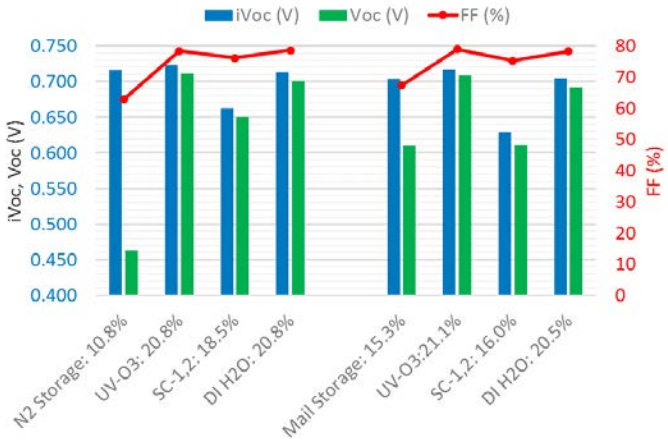

FIGURE 4. Device iV_{oc} and V_{oc} and FF after SiO_2 storage in an N_2 environment with and without post storage treatments.

It is well known that boron increases hydrogen effusion from amorphous silicon[7]. Additionally, during a-Si:H deposition, a near-surface hydrogenated layer will form on a silicon substrate but not on a glass substrate[8]. For specific growth conditions, this hydrogen reservoir will also concurrently release hydrogen during the deposition or subsequent thermal treatment, resulting in blistering of the a-Si:H on Si but not on the glass. While this may partially explain the presence of the blisters in our devices, blistering was not observed in the treated samples, so hydrogen effusion and coalescence are not the sole causes for blister induced degradation.

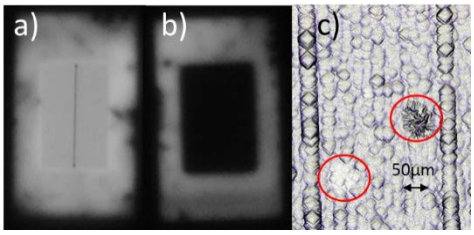

FIGURE 5. Photoluminescence images of UV-O_3 a) treated and b) untreated cells after storage for a week. Blisters (red circles in c) in the p/poly-Si layer.

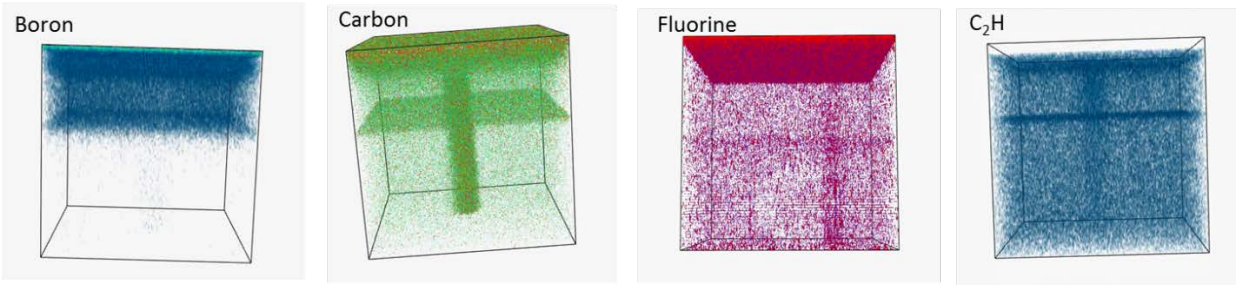

FIGURE 6. ToF-SIMS tomographic mapping of intact blister though p/poly-Si (top) passivated contact structure on SiO2 (middle line) capped cSi wafer (bottom).

ToF-SIMS tomographic mapping (figure 6) through an intact ~30 µm blister shows that boron, carbon, fluorine, and C_2H can clearly be seen on the SiO_2/poly-Si interface as well as coalesced in the blister itself, realized by the cylindrical shape in the figures. During the high temperature crystallization anneal, localized weak adhesion points at the interface created conditions favorable for mobile elements to migrate. As they continue to diffuse and collect, the blister gets larger, but the SiO_2 remains intact on the cSi.

When comparing surface spectra (figure 7) of stored-and-treated versus stored-and-untreated tunneling SiO_2, we find polypropyelene fragmentations[9] at atomic mass of ~288.3 as a result of the container in which we store our samples. These adhere to the SiO_2 layer to create the localized weak attachment points for the a-Si:H. Environmental conditions such as containment and latent chemistry, even in a cleanroom, are well known to contaminate surfaces[10,11]. Once the delamination has nucleated, the action of boron enhanced hydrogen effusion as well as contaminant migration produce growing blisters. This results in a final blistered p/poly-Si layer that will allow recombination-active direct metal contact to the cSi absorber.

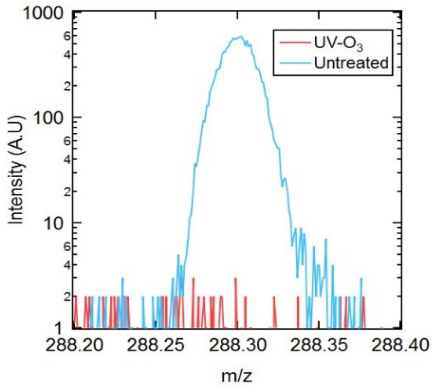

FIGURE 7. ToF-SIMS Surface spectra with polypropylene fragment signal on untreated SiO_2 surface

CONCLUSIONS

We find that environmental contaminants resulting from storing our tunneling SiO_2 in polyprolylene containers in a clean room result in blisters only in the p/poly-Si layer, but not i/ or n/poly-Si of our devices. The mechanism for blister growth occurs by hydrocarbons adhering to the SiO_2 locally creating weak attachment points during a-Si:H deposition. The subsequent anneal into poly-Si reveals the segregation of hydrogen, boron, and carbon to blisters. This leads to eventual recombination active direct metal contact to the underlying cSi absorber. Treatments to the stored SiO_2 layer such as UV-O_3 exposure and even a deionized water dip result in >20% front/back all poly-Si passivated contact cells. The treatments do not cause SiO_2 growth as evidenced by fill factors ~78%.

REFERENCES

1. K. Yoshikawa, Y. Wataru, T. Irie, H. Kawasaki, K. Konishi, H. Ishibashi, T. Asatani, D. Adachi., M. Kanematsu, H. Uzu. and K.Yamamoto, Solar Energy Materials and Solar Cells 173, 37-42 (2017).
2. D. Smith, G. Reich, M. Baldrias, M. Reich, N. Boitnott, and G. Bunea, "Silicon solar cells with total area efficiency above 25%." Proceedings of the 43rd IEEE Photovoltaic Specialists Conference, Portland, OR, USA, 2016, pp. 3351-3355.
3. G. Nogay, A. Ingenito, E. Rucavado, Q. Jeangros, J. Stuckelberger, P. Wyss, M. Morales-Masis, F.Haug, P. Löper, and C. Ballif, IEEE Journal of Photovoltaics 99, 1-8 (2018).
4. T. Aoyama, K. Suzuki, H. Tashiro, Y. Toda, T. Yamazaki, K. Takasaki, and T. Ito, Journal of Applied Physics 77 (1), 417-419 (1995).
5. S. Bakhshi, N. Zin, H. Ali, M. Wilson, D. Chanda, K. Davis, and W. Schoenfeld, Solar Energy Materials and Solar Cells 185, 505-510 (2018).
6. M. Heyns, S. Verhaverbeke, M. Meuris, P. Mertens, H. Schmidt, M. Kubota, A. Philipossian, K. Dillenbeck, D. Graf, A. Schnegg, and R. De Blank, "New wet cleaning strategies for obtaining highly reliable thin oxides," MRS Online Proceedings Library Archive 315 (1993).
7. W. Beyer, and H. Wagner, *Le Journal de Physique Colloques* 42. C4-783 (1983).
8. R. Rao, F. Kail, and P. Roca i Cabarrocas, Journal of Materials Science: Materials in Electronics 18.10 1051-1056 (2007).
9. M. Aznar, A. Rodriguez-Lafuente, P. Alfaro, and C. Nerin, Analytical and Bioanalytical Chemistry, 404(6-7), 1945-1957 (2012).
10. S. De Gendt, D.M. Knotter, K. Kenis, M. Depas, M. Meuris, P.W. Mertens, and M.M. Heyns, Japanese Journal of Applied Physics, 37(9R), 4649. (1998).
11. H. Yamazaki, M. Tamaoki, and M. Oohashi, Japanese Journal of Applied Physics, 39(8R), 4744 (2000).